Supplementary Information (SI) for Environmental Science: Nano.

The Bimetallic Effect between Pd and Rh on the Hydrodefluorination Activity of RhPd/TiN: Mechanism study and Implication to Simultaneously Removal of Multiple Halogenated organics

Peihong Li[1,2], Xiaoling Zhang[1,3], Zhineng Hao[1,3] and Rui Liu[*1,2,3]

1. State Key Laboratory of Environmental Chemistry and Ecotoxicology, Research Center for Eco-Environmental Sciences, Chinese Academy of Sciences, Beijing 100085, China

2. School of Environment, Hangzhou Institute of Advanced Study, UCAS, Hangzhou, 310024 China

3. College of Resources and Environment, University of Chinese Academy of Sciences, Beijing, 100049, China

Corresponding author: ruiliu@rcees.ac.cn

This supporting information contains 27 pages: about 12 pages of text, 3 tables, 24 figures and 3 cited literatures.

Table of content

1. Synthesis of nanocatalysts

1.1 Materials and Chemicals

Na_2PdCl_4 and $TiCl_4$ were purchased from Sigma-Aldrich Trading Co., Ltd. (Shanghai, China). $RhCl_3 \cdot 3H_2O$, 4-fluorophenol (4-FP), TiO_2, phenol, cyclohexanone (99.90%) and cyclohexanol (99%) were brought from Aladdin Biochemical Technology Co., Ltd. (Shanghai, China). Ethanol, KBH_4, NaOH, HCl, HNO_3 and $NH_3 \cdot H_2O$ (25.0%-28.0%) were supplied from Sinopharm Chemical Reagent Co., Ltd. (Beijing, China). Methyl alcohol, dichloromethane and n-hexane were purchased from Energy Chemical (Shanghai, China).

1.2 Synthesis of TiN support

TiN nanoparticles (TiN NPs) were synthesized according to our previously protocol using a complexation-nitridation method.[1] Typically, 1 mL titanium tetrachloride ($TiCl_4$) was dissolved in 30 mL of ethanol under stirring. After mixing uniformly, NH_3 gas was introduced into the solution at a rate of 50 sccm for 30 min, yielding a white precipitate. Then, the precipitate was transferred to the vacuum oven at 85 °C overnight. The obtained solid was then placed in the tube furnace and heated at 800°C for 3 h under the NH_3 atmosphere (50 sccm) and the heating rate during the calcination process in an NH_3 atmosphere was 5 °C/min. Then cooled to room temperature by the protection of the argon atmosphere.

For the TiN microparticles (TiN MPs), hydrothermal synthesis method was used. First, 1 mL $TiCl_4$ was dissolved into 40 mL 1-octanol under the continuous stirring for 30 min to form a uniformly solution. Then, the solution was transferred to an 80 mL Teflon lined stainless steel autoclave and heated to 150°C for 12 h. Then, the obtained sediment was centrifugated at 5000 rpm and washed by ethanol three times, and the dried at 85°C overnight. The solid

was nitride at 800°C for 8 h under the NH_3 atmosphere (50 sccm) in the tube furnace

1.3 Synthesis of RhPd/TiN

RhPd/TiN catalysts were synthesized via KBH_4 reduction of pre-adsorbed Rh^{3+} and $PdCl_4^{2-}$ with varying Rh and Pd loadings (0.05, 0.1, 0.2, 0.5, 1.0, 2.0 wt%). For example, to prepare 0.5 wt% Rh_1Pd_1/TiN, $NaPdCl_4$ (0.25 mL, 5 mM) and $RhCl_3$ (0.25 mL, 5 mM) were mixed in different proportions to create Rh (Ⅲ)+Pd (Ⅱ) precursors solution with a range of Rh/Pd molar ratios. Then, 50 mg TiN powder was dispersed into 20 mL deionized H_2O. After ultrasonication for 30 min, the mixed-precursors solution was added to the suspension in ice bath under 600 rpm stirring. Subsequently, the freshly prepared KBH_4 (5 mL, 1.7 $mg \cdot mL^{-1}$) was added dropwise to the suspension. The samples were separated by centrifugation at 5000 rpm and washed with deionized water twice to remove any impurities. The final 0.5 wt% Rh_1Pd_1/TiN nanocomposites were vacuum dried overnight at 85°C and stored for the sequent experiment.

1.4 Synthesis of RhPd/TiN in a stepwise manner

The synthesis of Rh+Pd/TiN_{Pd} (depositing Rh and the pre-synthesized Pd/TiN) and Pd+Rh/TiN_{Rh} (depositing Pd on the pre-synthesized Rh/TiN) are similar to RhPd/TiN. Firstly, for Rh+Pd/TiN_{Pd}, 50 mg TiN powder was dispersed into 20 mL deionized H_2O and with ultrasonic action for 30 min. Then, the suspension was placed in ice bath and $NaPdCl_4$ (0.08 mL, 5 mM) was added dropwise to the suspension under 600 rpm stirring. After 15 min stirring, the freshly prepared KBH_4 (5 mL, 1.7 $mg \cdot mL^{-1}$) was added dropwise to the suspension and got the Pd/TiN catalyst. Subsequently, $RhCl_3$ (0.12 mL, 5 mM) was added dropwise to the suspension and stirred for 1 h. The solid sample was Rh+Pd/TiN_{Pd}. For Pd+Rh/TiN_{Rh}, it only needs to exchange the order of adding $RhCl_3$ and $NaPdCl_4$, and the rest of the steps are the same as above

1.5 Synthesis of control catalysts

1.5.1 Synthesis of Rh_3Pd_2/TiO_2-0.2

The synthesis of Rh_3Pd_2/TiO_2-0.2 is similar to that for RhPd/TiN. Briefly, $NaPdCl_4$ (0.12 mL, 5 mM) and $RhCl_3$ (0.08 mL, 5 mM) were mixed to create Rh (Ⅲ)+Pd (Ⅱ) precursors solution with a range of Rh/Pd molar ratios. Then, 50 mg TiO_2 powder was dispersed into 20 mL deionized H_2O. After ultrasonication for 30 min, the mixed-precursors solution was added to the suspension in ice bath under 600 rpm stirring. Subsequently, the freshly prepared KBH_4 (5 mL, 1.7 $mg \cdot mL^{-1}$) was added dropwise to the suspension. The samples were separated by centrifugation at 5000 rpm and washed with deionized water twice to remove any impurities. The final 0.2 wt% Rh_3Pd_2/TiO_2 nanocomposites were vacuum dried overnight at 85°C and stored for the sequent experiment.

1.5.2 Synthesis of Rh_3Pd_2/SiO_2-0.2

In the first step, SiO_2 support was synthesized via Stöber method. 50 mL of ethanol, 1 mL of ultra-pure water and 4 mL of ammonia were taken into a conical bottle and stirred at 500 rpm. In the stirring state, 5 mL ethyl tetrasilicate (TEOS) was added drop by drop and continued to stir for 30 min. The transparent solution gradually turned into a milky white suspension, which was SiO_2 nanoparticles. Then, the white precipitate was taken by centrifuging at 5000 rpm and cleaned it with anhydrous ethanol for 3 times. Solid SiO_2 nanoparticles were obtained by heating and drying overnight at 85°C in a vacuum drying oven. Subsequently，50 mg SiO_2 nanoparticles were taken to prepare Rh_3Pd_2/SiO_2-0.2 and the method was the same as that for Rh_3Pd_2/TiO_2-0.2.

1.5.3 Synthesis of Rh_3Pd_2/SiN-0.2

The synthesis of Rh_3Pd_2/SiN-0.2 was similar to that for Rh_3Pd_2/TiO_2-0.2. A 50 mg portion of SiN nanoparticles was dispersed in 20 mL ultrapure water via

ultrasonication to achieve homogeneous dispersion. Under ice-bath conditions with vigorous stirring at 800 rpm, 0.12 mL of 5 mM $RhCl_3$ solution and 0.08 mL of 5 mM $NaPdCl_4$ solution were simultaneously introduced into the SiN suspension. Following complete homogenization, 5 mL of freshly prepared KBH_4 aqueous solution (1.7 mg·mL^{-1}) was rapidly injected into the mixture, yielding a gray colloidal suspension. The resultant suspension was subjected to centrifugation, after which the gray precipitate was collected, vacuum-dried at 85°C for 12 h, and preserved for subsequent characterization.

1.5.4 Synthesis of Rh_3Pd_2/Al_2O_3-0.2

Firstly, Al_2O_3 was synthesis via hydrothermal method.[2] Aluminum nitrate (6.44 g, $Al(NO_3)_3·9H_2O$) and urea (9.28 g, $CO(NH_2)_2$) were dissolved in ultrapure water under magnetic stirring for 25 min. The solution was transferred to a 180 mL Teflon-lined stainless-steel autoclave and hydrothermally reacted at 100°C for 48 h. After cooling to room temperature, the white precipitate was collected, washed repeatedly with ultrapure water and ethanol, and dried at 80°C for 10 h. The powder was calcined in air at 600°C for 2 h (1 °C/min) to obtain Al_2O_3 nanoparticles. Then，50 mg Al_2O_3 nanoparticles were taken to prepare Rh_3Pd_2/Al_2O_3-0.2 and the method was the same as that for Rh_3Pd_2/TiO_2-0.2.

1.5.5 Synthesis of Rh_3Pd_2/C-0.2

The synthesis of Rh_3Pd_2/C-0.2 was similar to that for Rh_3Pd_2/TiO_2-0.2. In detailly, A 50 mg portion of conductive carbon black was ultrasonically dispersed in a mixed solvent containing 20 mL ultrapure water and 20 mL anhydrous ethanol. Under ice-bath conditions with vigorous stirring at 800 rpm, a mixture of 0.12 mL 5 mM $RhCl_3$ solution and 0.08 mL 5 mM $NaPdCl_4$ solution was introduced into the dispersion. After complete homogenization, 5 mL of freshly prepared KBH_4 aqueous solution (1.7 mg·mL^{-1}) was rapidly injected into the system. The black precipitate was isolated via centrifugation, vacuum-dried

at 85°C for 12 h, and preserved for subsequent characterization.

2. Catalysis Experiment

The catalytic performance of RhPd/TiN for hydrodefluorination of 4-FP was evaluated as follows: A mixture of 27 mL ultrapure water and 1 mL 30 mM 4-FP aqueous solution was prepared in a 50 mL conical flask. The pH was adjusted to 8–9 by adding 1 mL 45 mM NaOH solution, and the system was continuously stirred at 450 rpm on a magnetic stirrer. H_2 gas (100 mL·min^{-1}) was continuously supplied via a hydrogen generator to the reaction mixture. After stabilizing the H_2 flow, 1 mL catalyst (total Rh and Pd molar concentration: 0.6 mM) was injected, achieving a 4-FP-to-bimetallic Rh/Pd molar ratio of 50:1. Aliquots were periodically collected at specified time intervals using a syringe filtered through a 0.22 μm pore-size membrane.

3. Characterizations of the Catalysts

Transmission electron microscopy (TEM) and high-resolution transmission electron microscopy (HRTEM) characterizations were performed using a JEM-2100F field-emission electron microscope (JEOL Ltd., Tokyo) operated at 200 kV accelerating voltage. Spherical aberration-corrected high-angle annular dark-field scanning transition electron microscopy (Cs-HAADF-STEM) combined with energy-dispersive X-ray spectroscopy (EDX) elemental mapping was conducted on a JEM-ARM200F atomic resolution analytical microscope (JEOL, Japan) equipped with a cold field-emission gun. X-ray photoelectron spectroscopy (XPS) measurements were acquired through a Kratos AXIS ULTRADLD spectrometer (Kratos Analytical Ltd., UK) employing monochromatic Al Kα radiation (1486.6 eV), with binding energies calibrated against the C 1s peak at 284.8 eV. All specimens were prepared by drop-casting ethanol-dispersed samples onto carbon-coated copper grids.

4. Loading efficient analysis

To determine the Rh and Pd loading efficiency on TiN, all catalysts were analyzed by ICP-MS (Agilent 8900, USA) following aqua regia digestion. Specifically, 1.0 mL catalyst suspension was digested with 3 mL aqua regia for 2 h, then diluted 1000-fold with 5% nitric acid prior to ICP-MS measurement. As summarized in Table S1, the actual Rh/Pd loadings (0.05, 0.1, 0.2, 0.5, 1.0, 2.0%) and molar ratios closely matched theoretical values, confirming successful growth of Rh-Pd alloys on TiN nanoparticles. This controlled loading range validates their suitability for systematic catalytic studies.

Table S1. Theoretical and experimental loading test results table of RhPd/TiN

Theoretical Ratio of Rh:Pd	Theoretical loading （wt%）	Experimental loading（wt%）	Theoretical Ratio of Rh/ (Rh + Pd)	Experimental Ratio of Rh/ (Rh + Pd)	Theoretical Ratio of Pd/ (Rh + Pd)	Experimental Ratio of Pd/ (Rh + Pd)
1:16	0.20	0.23	0.059	0.062	0.941	0.938
1:10	0.20	0.16	0.091	0.096	0.909	0.904
1:8	0.20	0.21	0.111	0.129	0.889	0.871
1:5	0.20	0.23	0.167	0.172	0.833	0.828
1:2	0.20	0.20	0.333	0.353	0.667	0.647
1:1	0.20	0.20	0.500	0.517	0.500	0.483
3:2	0.20	0.18	0.600	0.597	0.400	0.403
2:1	0.20	0.20	0.667	0.663	0.333	0.337
3:2	0.05	0.05	0.600	0.607	0.400	0.393
3:2	0.10	0.11	0.600	0.603	0.400	0.397
3:2	0.20	0.21	0.600	0.617	0.400	0.383
3:2	0.50	0.51	0.600	0.609	0.400	0.391
3:2	1.00	0.97	0.600	0.583	0.400	0.417
3:2	2.00	1.94	0.600	0.597	0.400	0.403

5. Hydrogen spillover detection by WO_3

A mixture of 50 mg catalysts ang 500 mg WO_3 was put in a tube furnace and kept at 50℃ for 1 h in an H_2 flow (100 $mL \cdot min^{-1}$).[3] Then, the colors of the mixture before and after H_2 treatment were pictured for comparison.

6. RhPd/TiN Microparticle-Based Water Treatment Column

The water treatment column was initially sealed with a sand core filter. Subsequently, 200 mg of synthesized Rh_3Pd_2/TiN-0.2 microparticles (MPs) were homogenously blended with 15 g quartz sand and packed into the column, establishing a fixed-bed reactor with 6.6 mL bed volume (BV). Two aqueous matrices were prepared:

1) Water sample was collected from the Xiaoyue River (Beijing, China), with detailed physicochemical parameters listed in Table S2. The river water was filtered through 0.22 μm membranes to remove macroscopic impurities and microbial communities. Then, the sample was spiked with equimolar concentrations (0.02 mM each) of 4-fluorophenol (4-FP), 4-chlorophenol (4-CP), 4-bromophenol (4-BP), and 4-iodophenol (4-IP) as simulated wastewater.

Table S2. Parameters of river water employed as simulated water sample for the treatment of halogenated wastewater.

Parameter	Content	Concentration
pH	7.97	
Carbon (mg L^{-1})	Total carbon	44.39
	Total inorganic carbon	33.79
	Total organic carbon	10.61
Anion (mM)	Cl^-	2.25
	SO_4^{2-}	0.99
Cation (mM)	K^+	0.15
	Na^+	2.24
	Ca^{2+}	1.64
	Mg^{2+}	1.73

2) The industrial wastewater was sourced from a pharmaceutical manufacturing plant in China, with detailed physicochemical parameters listed in Table S3. The collected pharmaceutical effluent was filtered through 0.22 μm membranes to eliminate macroscopic particulates and organic constituents. Both matrices were filtered through 0.45 μm membranes to eliminate particulates and microbiota. A peristaltic pump delivered the solutions through the column at 4.5 mL·min^{-1}, with 5 min·BV^{-1} hydraulic retention time regulated via H_2 pressure adjustment.

Table S3. Parameters of the industrial wastewater employed as simulated water sample for the treatment of pharmaceutical wastewater.

Parameter	Content	Concentration
pH	7.37	
Carbon (mg L^{-1})	Total carbon	369.5
	Total inorganic carbon	255.3
	Total organic carbon	114.1
Anion (mM)	Cl^-	2.73
	SO_4^{2-}	1.21
Cation (mM)	K^+	2.1
	Na^+	2.21
	Ca^{2+}	1.78
	Mg^{2+}	1.71

7. Additional Figures

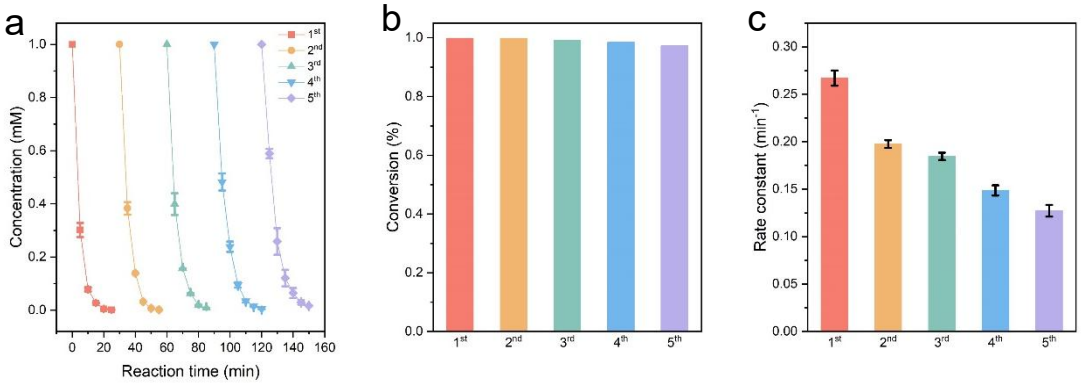

Figure S1. The stability test of Rh_3Pd_2/TiN-0.2 in the HDF of 4-FP. (a, b) Conversion profiles of 4-FP catalyzed by Rh_3Pd_2/TiN for five uses. (c) Calculated rate constant for Rh_3Pd_2/TiN for five uses.

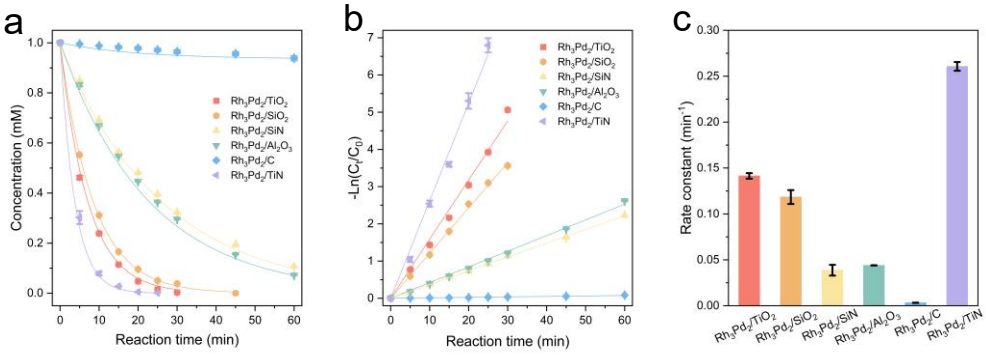

Figure S2. Catalysis performance of the catalysts with different supports in the HDF of 4-FP. (a) Conversion profiles of 4-FP catalyzed by the catalysts with different supports. (b, c) First-order kinetics data and calculated rate constant for different catalysts.

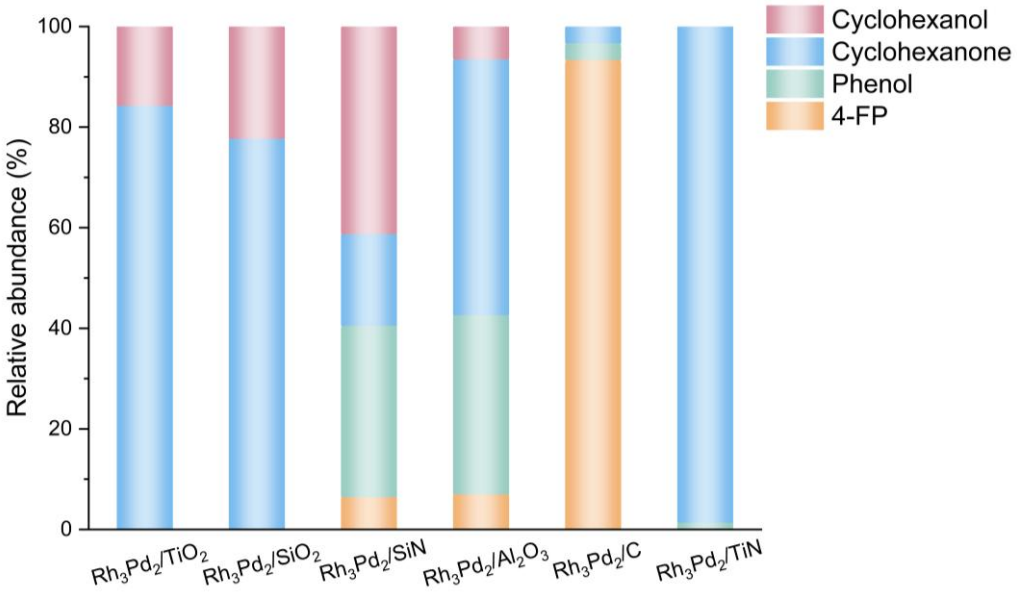

Figure S3. Relative abundance of the products in the HDF of 4-FP catalyzed by different loading.

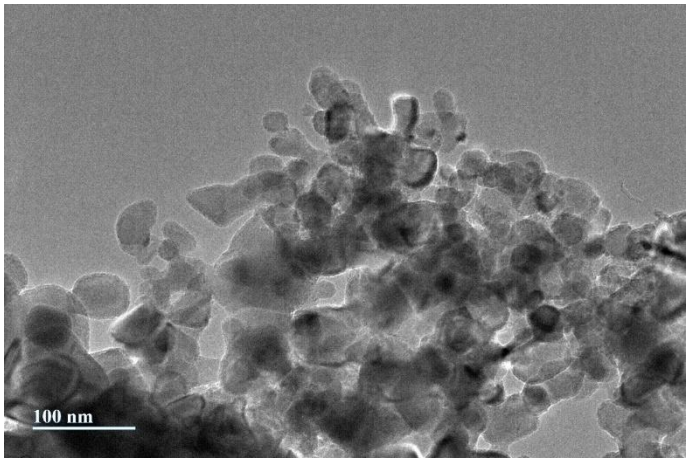

Figure S4. TEM images of TiN.

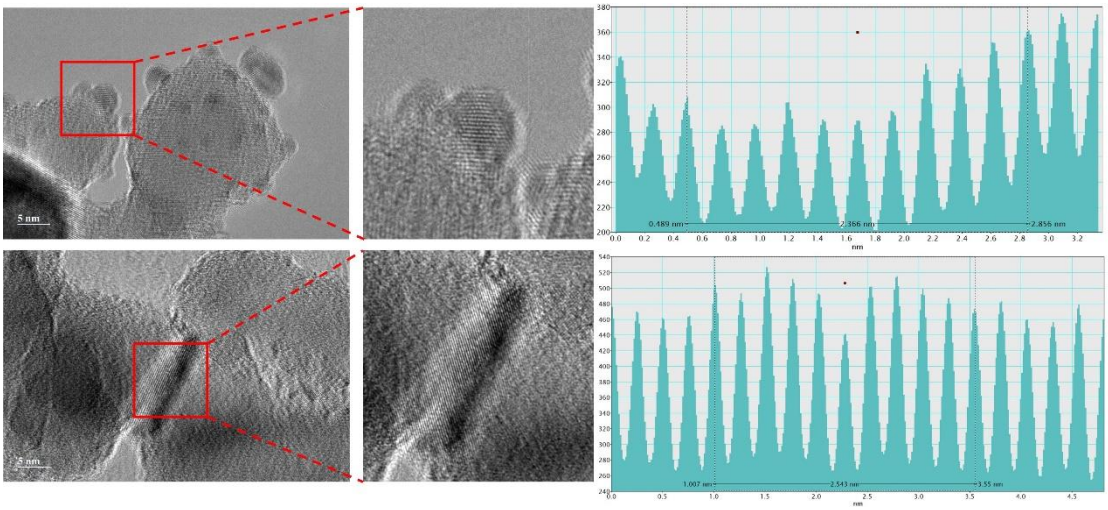

Figure S5. Structural characterization of Rh and Pd nanoparticles and TiN. (a, b, d, e) TEM images of RhPd nanoparticles and TiN; (c, f) RhPd nanoparticles and TiN lattice spacing measurements.

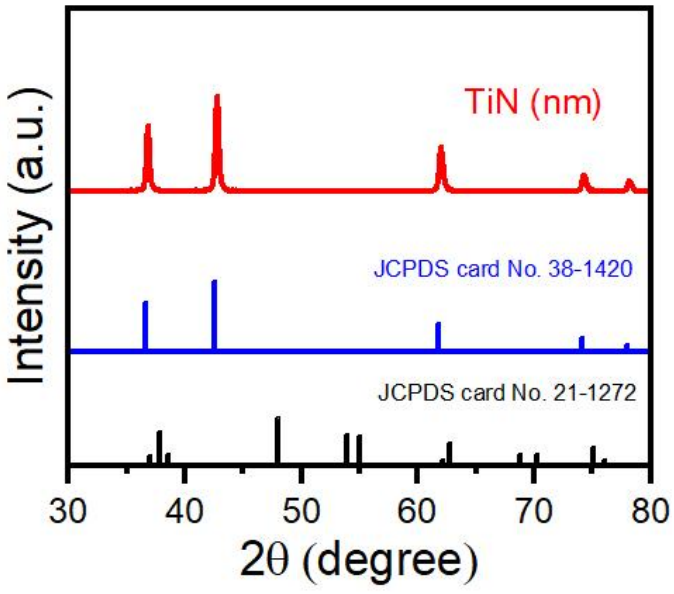

Figure S6. XRD patterns of nano TiN.

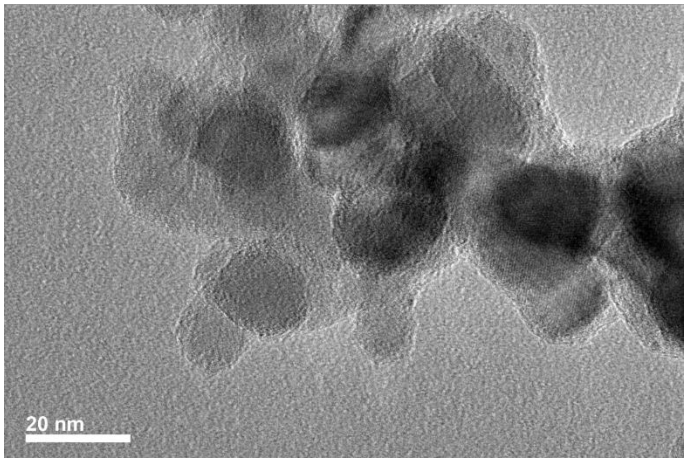

Figure S7. TEM images of Rh_3Pd_2/TiN-0.05.

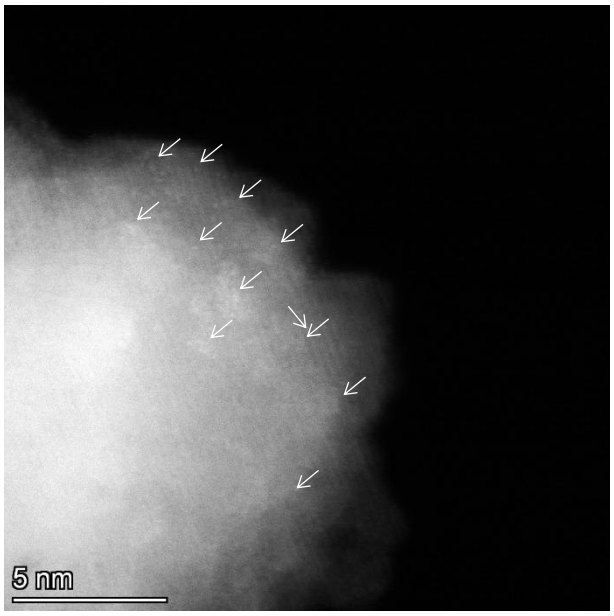

Figure S8. Cs-HAADF-STEM images of Rh_3Pd_2/TiN-0.05. The single-atom Rh-Pd sites are marked with white arrows.

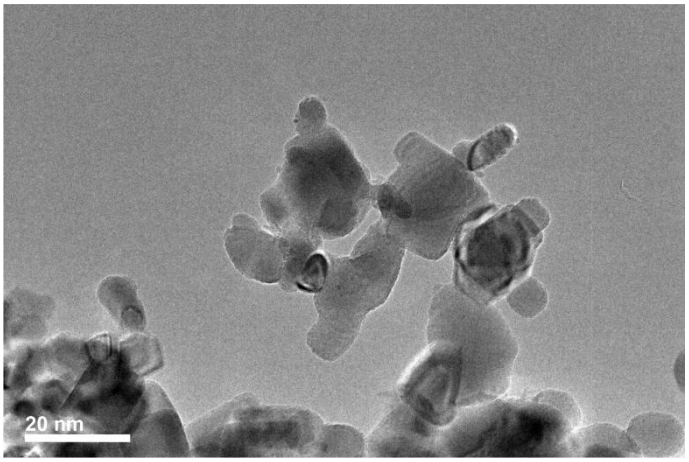

Figure S9. TEM images of Rh_3Pd_2/TiN-0.1.

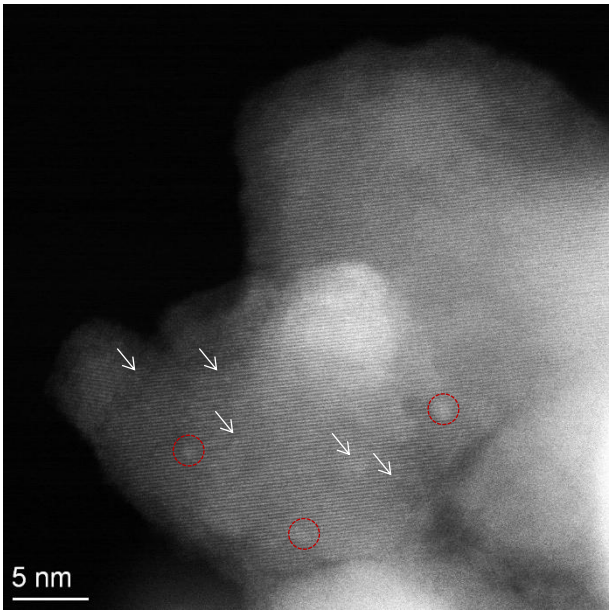

Figure S10. Cs-HAADF-STEM images of Rh_3Pd_2/TiN-0.1. The single-atom Rh-Pd sites are marked with white arrows. Rh-Pd ensembles are marked with red circles.

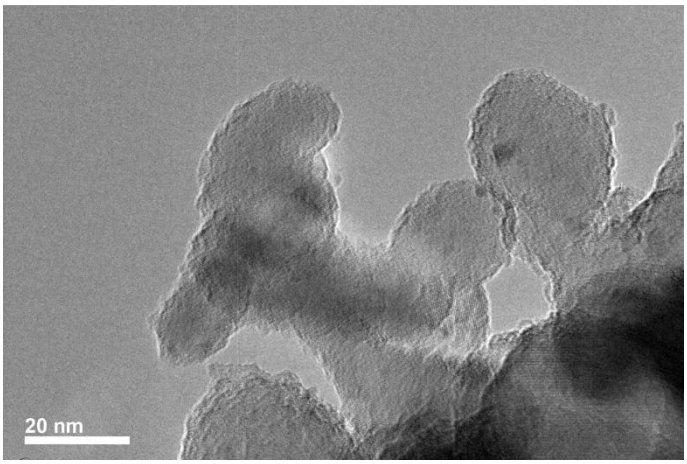

Figure S11. TEM images of the Rh_3Pd_2/TiN-0.5.

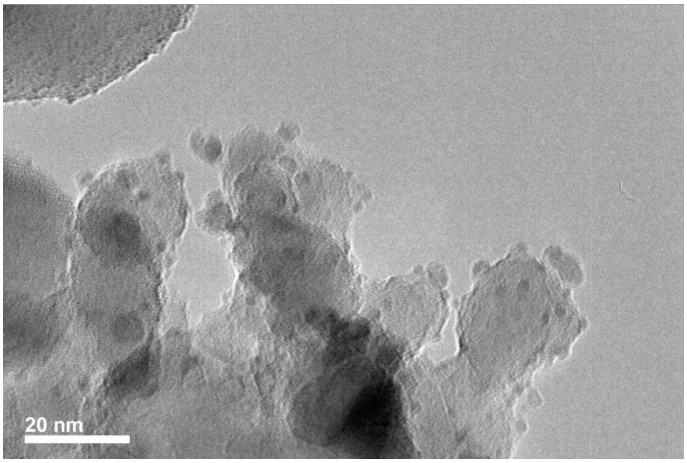

Figure S12. TEM images of the Rh_3Pd_2/TiN-1.0.

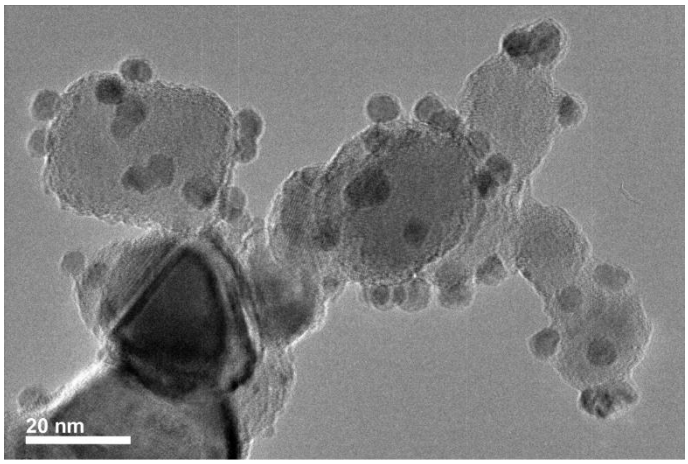

Figure S13. TEM images of the Rh_3Pd_2/TiN-2.0.

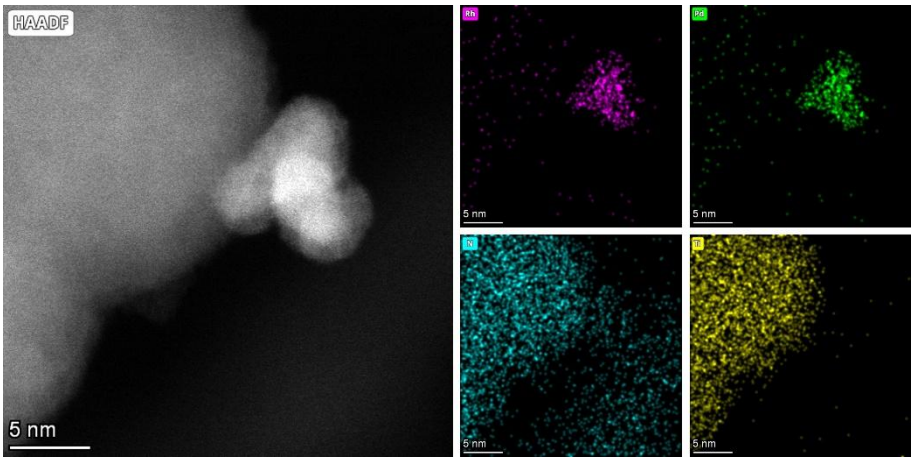

Figure S14. Cs-HAADF-STEM and EDX mapping images of Rh_3Pd_2/TiN-2.0.

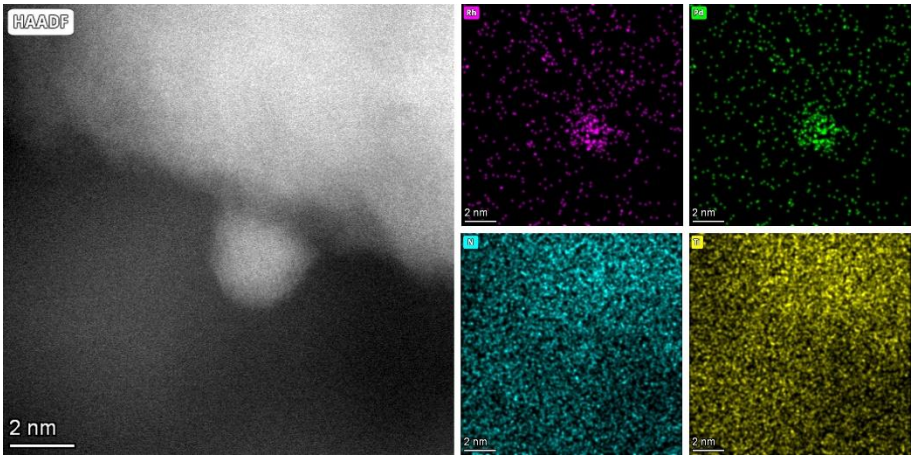

Figure S15. Cs-HAADF-STEM and EDX mapping images of Pd+Rh/TiN_{Rh}.

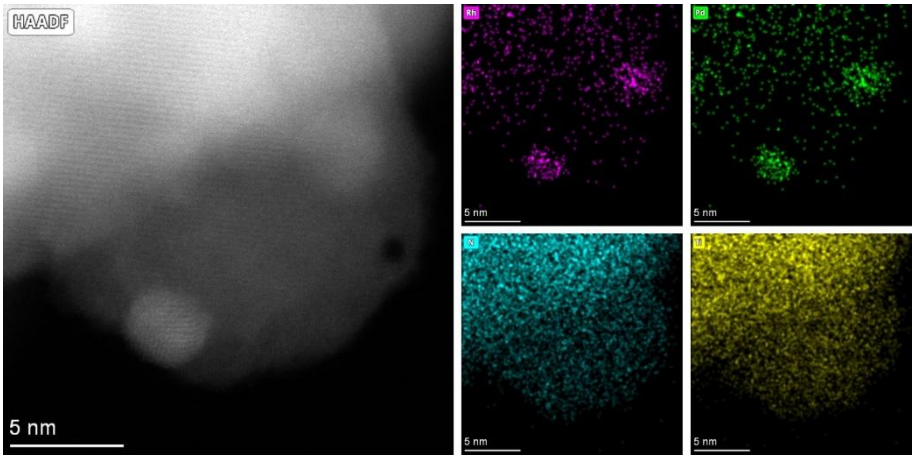

Figure S16. Cs-HAADF-STEM and EDX mapping images of Rh+Pd/TiN_{Pd}.

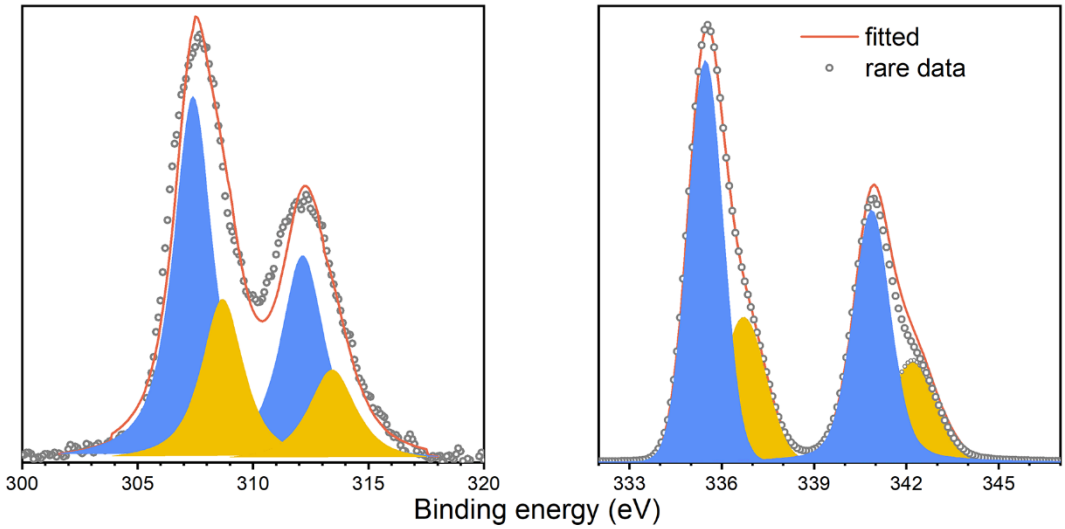

Figure S17. High-resolution XPS Rh 3d and Pd 3d spectra of the Rh_3Pd_2/TiN-1.0.

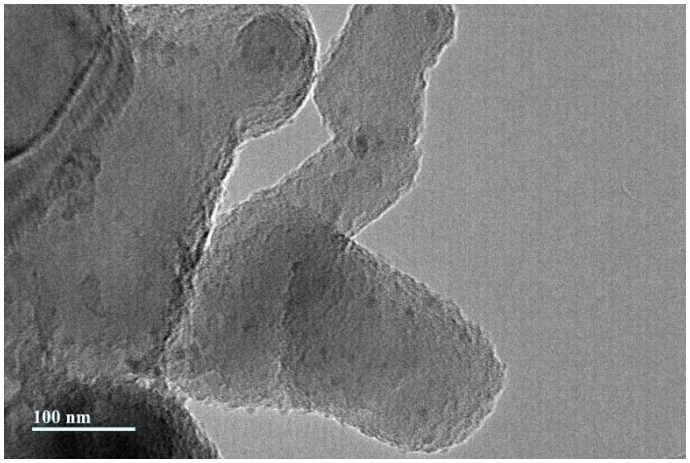

Figure S18. TEM of Rh_3Pd_2/TiN MPs

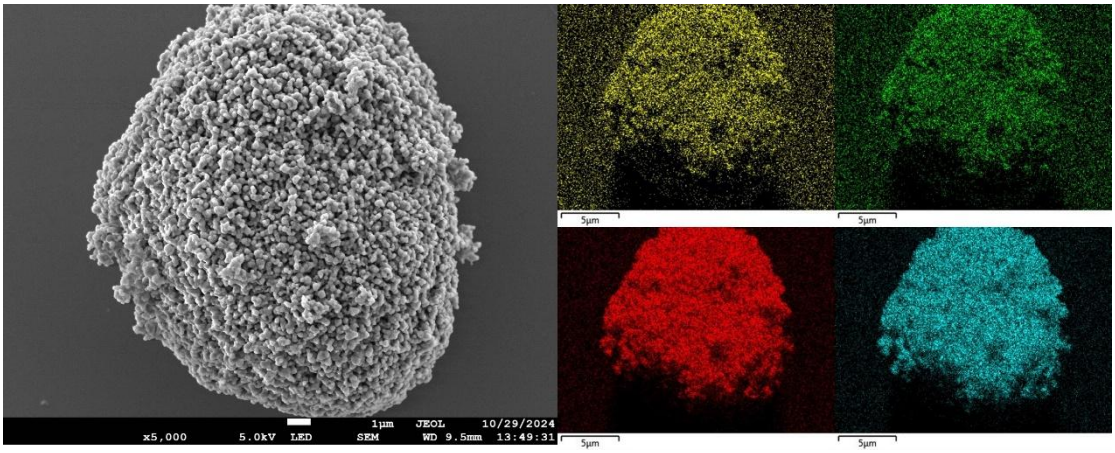

Figure S19. EDS elemental mapping of Rh_3Pd_2/TiN MPs.

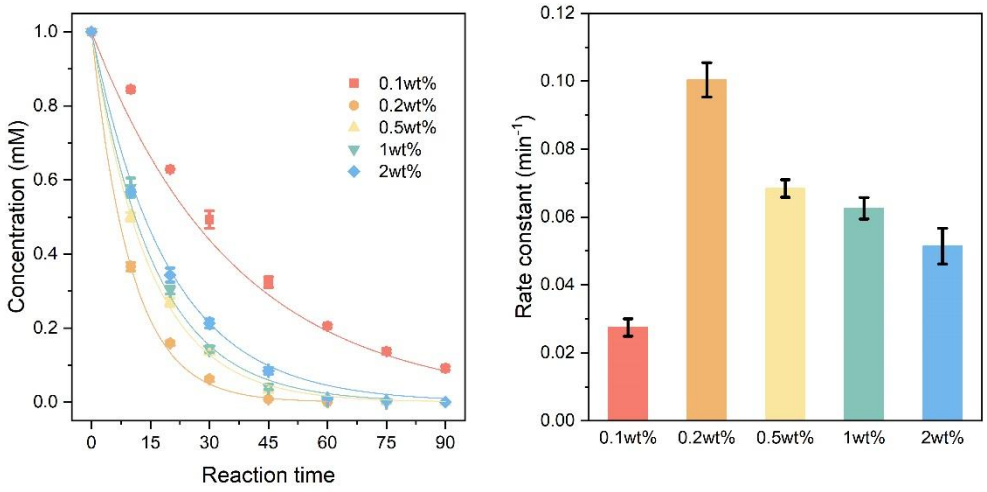

Figure S20. Catalysis performance of Rh_3Pd_2/TiN in the hydrodefluorination of 4-FP. (a) Conversion profiles of 4-FP catalyzed by the catalyst of micro Rh_3Pd_2/TiN with different loading. (b) Calculated rate constant for different catalysts.

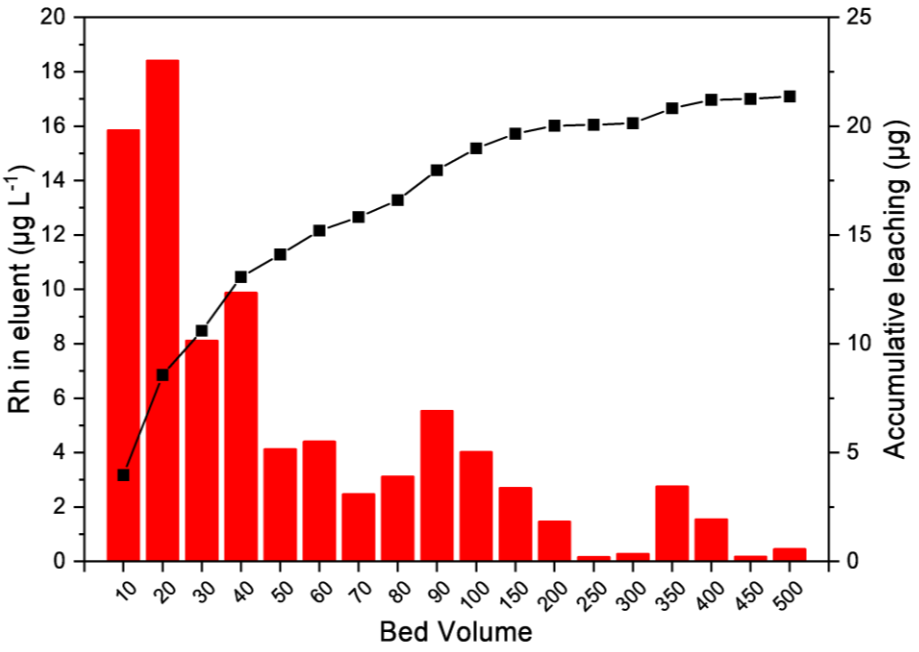

Figure S21. The leaching Rh into the eluent during the treatment of 500 BV halogenated wastewater.

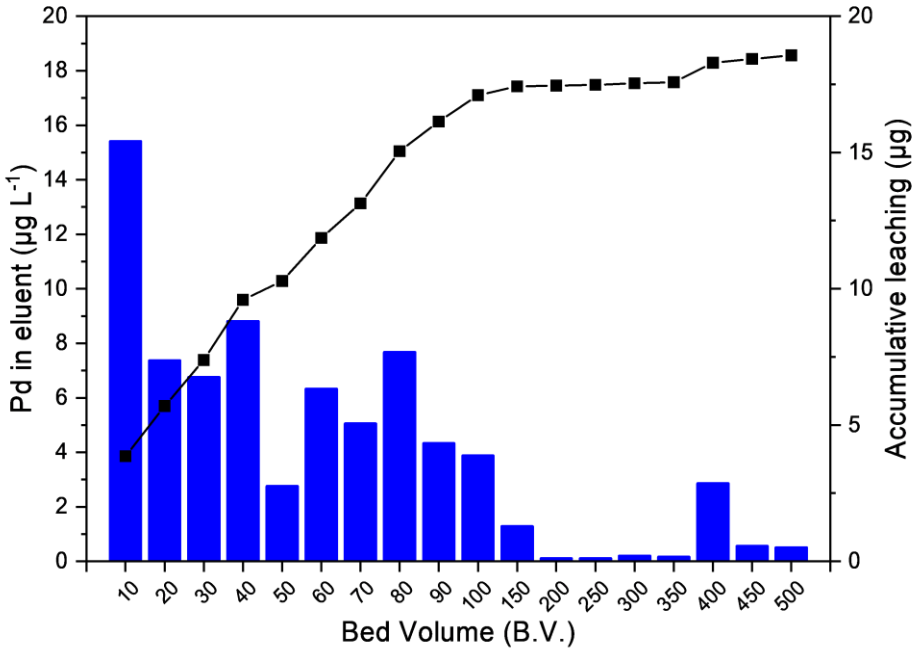

Figure S22. The leaching Pd into the eluent during the treatment of 500 BV halogenated wastewater.

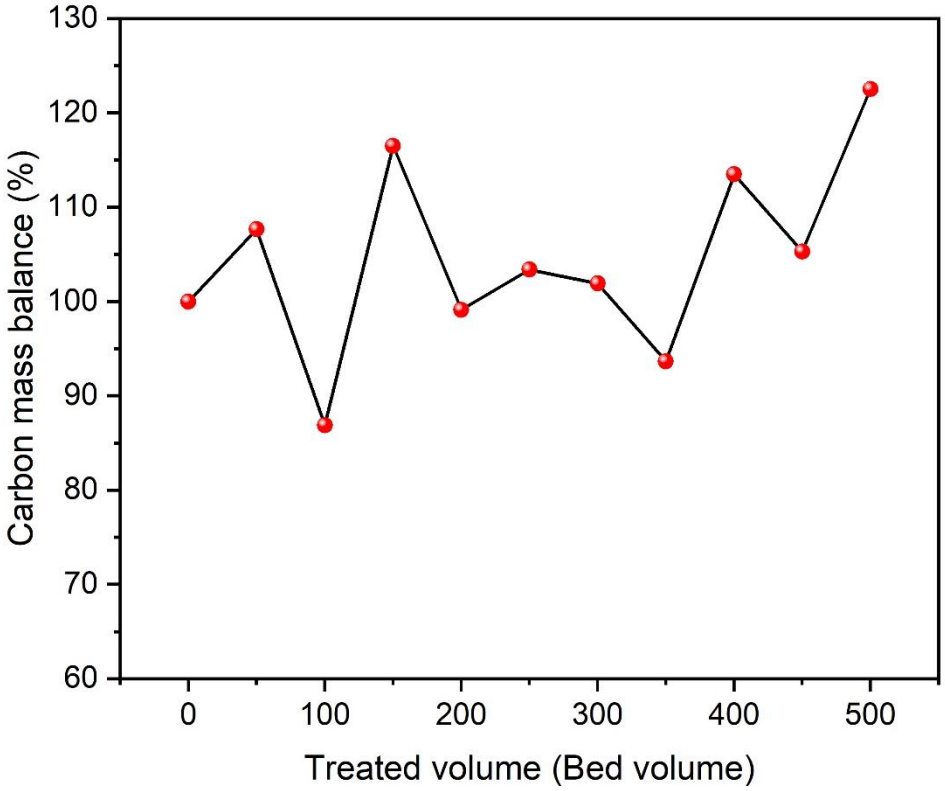

Figure S23. The carbon mass balance during the longtime treatment of 500 BV halogenated wastewater.

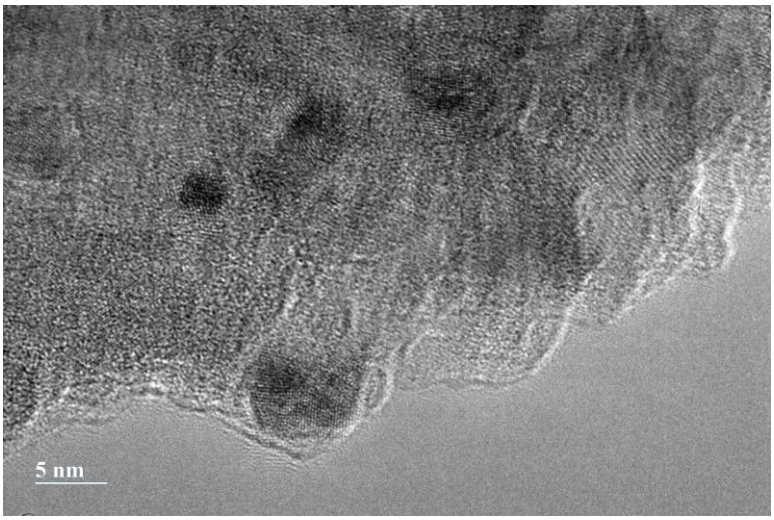

Figure S24. TEM of Rh_3Pd_2/TiN-0.2 after the stability test.

9. Reference

(1) Wang, W.; Zhang, X.; Ran, W.; Ma, C.; Sun, J.; Zhao, M.; Pan, W.; Liu, J.; Liu, R.; Jiang, G. Improving the Chemical Utilization Efficiency of Pd Hydrodechlorination Catalysts through Hydrogen-Spillover Empowered Synergy between Pd and TiNiN Support. *Environ. Sci. Technol*. **2024**, 58 (48), 21350-21361.

(2) Shi, L.; Deng, G.-M.; Li, W.-C.; Miao, S.; Wang, Q.-N.; Zhang, W.-P.; Lu, A.-H. Al_2O_3 Nanosheets Rich in Pentacoordinate Al^{3+} Ions Stabilize Pt-Sn Clusters for Propane Dehydrogenation. *Angew. Chem. Int. Ed*. **2015**, 54 (47), 13994-13998.

(3) Zhang, Y.; Zhan, S.; Liu, K.; Qiao, M.; Liu, N.; Qin, R.; Xiao, L.; You, P.; Jing, W.; Zheng, N. Heterogeneous Hydrogenation with Hydrogen Spillover Enabled by Nitrogen Vacancies on Boron Nitride-Supported Pd Nanoparticles. *Angew. Chem. Int. Ed.* **2023**, 62 (9), e202217191.